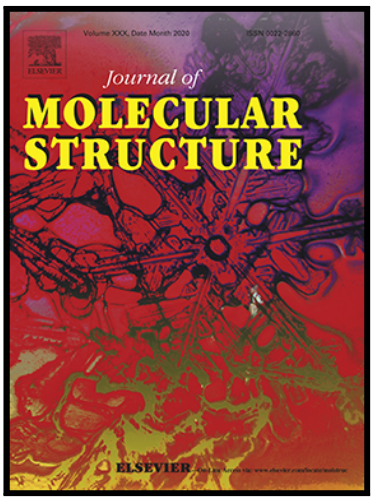

Synthesis, X-Ray Structure, Tautomerism Aspect, and Chemical Insight of The 3-(1H-Indol-2-yl)-7H-[1,2,4]triazolo[3,4-b][1,3,4]thiadiazin-6-ol

Ahmed T.A. Boraei , Matti Haukka , Saied M. Soliman , Assem Barakat

PII: S0022-2860(20)31744-0
DOI: https://doi.org/10.1016/j.molstruc.2020.129429
Reference: MOLSTR 129429

To appear in: *Journal of Molecular Structure*

Received date: 22 August 2020
Revised date: 6 October 2020
Accepted date: 7 October 2020

Please cite this article as: Ahmed T.A. Boraei , Matti Haukka , Saied M. Soliman , Assem Barakat , Synthesis, X-Ray Structure, Tautomerism Aspect, and Chemical Insight of The 3-(1H-Indol-2-yl)-7H-[1,2,4]triazolo[3,4-b][1,3,4]thiadiazin-6-ol, *Journal of Molecular Structure* (2020), doi: https://doi.org/10.1016/j.molstruc.2020.129429

Highlights

- A new triazolyl-indole was synthesized and characterized.
- Its low temperature X-ray single crystal structure was presented.
- Analysis of intermolecular interactions was performed using Hirshfeld calculations.
- DFT calculations were utilized to predict its electronic and spectroscopic aspects.
- The compound exists exclusively in the enol form.

Synthesis, X-Ray Structure, Tautomerism Aspect, and Chemical Insight of The 3-(1*H*-Indol-2-yl)-7*H*-[1,2,4]triazolo[3,4-*b*][1,3,4]thiadiazin-6-ol

Ahmed T. A. Boraei[1,*], Matti Haukka [3], Saied M. Soliman [3,*], and Assem Barakat [4,*]

[1] Chemistry Department, Faculty of Science, Suez Canal University, Ismailia 41522, Egypt.

[2] Department of Chemistry, University of Jyväskylä, P.O. Box 35, FI-40014 Jyväskylä, Finland, email: matti.o.haukka@jyu.fi (M.H.).

[3] Department of Chemistry, Faculty of Science, Alexandria University, P.O. Box 426, Ibrahimia, Alexandria 21321, Egypt. saied1soliman@yahoo.com & saeed.soliman@alexu.edu.eg (S.M.S).

[4] Department of Chemistry, College of Science, King Saud University, P. O. Box 2455, Riyadh 11451, Saudi Arabia.

***** Correspondence: E-mail: ahmed_boraei@science.suez.edu.eg; ahmed_tawfeek83@yahoo.com (A.T.A.B.); saied1soliman@yahoo.com (S.M.S); ambarakat@ksu.edu.sa(A.B.); Tel.: +966-11467-5901(A.B.); Fax: +966-11467-5992(A.B.).

Received: date; Accepted: date; Published: date

Abstract: The 3-(1*H*-indol-2-yl)-7*H*-[1,2,4]triazolo[3,4-*b*][1,3,4]thiadiazin-6-ol **2** was obtained exclusively in the enol configuration starting from triazolyl-indole derivative **1** and alkyl halo-esters in the presence of K_2CO_3. Chemical structure elucidations with the aid of physicochemical characterizations were used to predict its molecular structure while single crystal X-ray diffraction technique was used to shed the light on the supramolecular structure of **2**. DFT calculations agreed very well with the reported X-ray structure where the most stable form thermodynamically is the enol form. Its optimized geometry agreed very well with the experimental structure where the correlation coefficients between the calculated and experimental geometric parameters are very close to 1. Using Hirshfeld analysis, the most significant intermolecular contacts are the N…H, H…C(π), O…H, S…H and C…C contacts.

Keywords: triazolyl-indole; Tautomerism; Hirshfeld surface analysis; DFT; NBO.

1. Introduction

The 1,2,4-triazole motif connected to the indole scaffold have got remarkable attention in many pharmaceutical applications with diverse pharmacological effects [1,2]. Specifically, the 1,2,4-triazole-3-thione analogues with the amino-functionality in the fourth position have gain a lot of attention due to the presence of sulfur-nitrogen donor atoms which could bind to metals leads to enhancement of the pharmaceutical activity [3]. This scaffold system also can be employed as building blocks in a lot of chemical transformation including construction of Schiff bases and fused heterocycles [4,5]. Among the fused heterocyclic molecules is the s-triazolo[3,4-*b*]-1,3,4-thiadiazole and thiazolidines rings. In literature, this motif has diverse of biological properties in the recent years including anti-mycobacterial, antifungal, antimicrobial, antiviral, anticonvulsant, anti-HIV, anti-inflammatory, and anticancer activities [6-25].

On other hand, keto-enol tautomerism was studied extensively in literature because it plays a crucial role particularly in the biological systems. For example, DNA consist of nucleobases which exist exclusively in the keto tautomeric forms, mutations might be occurred if a single base converted from the keto form into the enol form [26]. To design, synthesize, and separate either of the two tautomer in a pure form is a challenge. A literature survey revealed that many of the fused heterocycles based s-triazolo[3,4-*b*]- thiazolidines rings were found in the keto-form [27-30]. Unfortunately, most of these findings are based on routine spectroscopic techniques and no X-ray structures were reported for these examples. In this text, we have been reported the synthesis of 3-(1*H*-indol-2-yl)-7*H*-[1,2,4]triazolo[3,4-*b*][1,3,4]thiadiazin-6-ol in the enol form. Additionally, the chemical insight of the synthesized compound was also investigated with the aid of different experimental and theoretical techniques.

2. Materials and Methods

All general notes regarding to the equipment's utilized in this study for structure elucidation have been provided in the Supplementary data.

2.1. Synthesis of the 3-(1H-indol-2-yl)-7H-[1,2,4]triazolo[3,4-b][1,3,4]thiadiazin-6-ol **2**

A mixture of triazolyl-indole derivative **1** (1.0 mmol) and potassium carbonate K_2CO_3 (1.2 mmol) dissolved in 10 mL EtOH (absolute) then allowed to stir for 1 h at rt. Subsequently, *tert*-butyl bromoacetate or ethyl chloroacetate (1.2 mmol) was added and the reaction mixture was refluxed for 3 h then cooled. Solvent was removed under reduced pressure, cold water has been added and the mixture was acidified with diluted HCl. The formed precipitate was filtered off, dried and recrystallized from EtOH or DMF/EtOH.

Yield: 81 %, m.p. 291-292 ^{o}C; ^{1}H NMR (DMSO-d_6, 300 MHz) δ 3.92 (s, 2 H, CH_2), 7.05 (dd, 1 H, $J_{4,5}$ 7.9, $J_{5,6}$ 7.3 Hz, H-5$_{Indole}$), 7.16-7.21 (m, 2 H, H-3$_{Indole}$, H-6$_{Indole}$), 7.45 (d, 1 H, $J_{6,7}$ 8.1 Hz, H-7$_{Indole}$), 7.64 (d, 1 H, $J_{4,5}$ 7.9 Hz, H-4$_{Indole}$), 11.90 (br. s, 1H, NH$_{Indole}$), 12.68 (br. s, 1 H, NH$_{Thiadiazine}$); ^{13}C NMR (DMSO-d_6, 75 MHz) δ 27.60 (*C*H$_{2Thiadiazine}$), 102.89 (C-3$_{Indole}$), 111.87 (C-7$_{Indole}$), 119.76 (C-5$_{Indole}$), 120.94 (C-4$_{Indole}$), 122.95 (C-2$_{Indole}$), 123.17 (C-6$_{Indole}$), 127.47 (C-3a$_{Indole}$), 136.71 (C-7a$_{Indole}$), 143.30, 144.61 (C-3$_{Triazole}$, C-5$_{Triazole}$), 164.23 (C=O), (Figs. S1-S4, Supplementary data); HRMS (EI) calcd for $C_{12}H_9N_5SO$ (M^+): 271.0552. Found: 271.0552.

2.2. Experimental method for X-Ray structure determinations

The experimental method for mounting the crystal along with the software package [31-33] to solve the data have been provided in the Supplementary data. Table 1 listed the data of the solid-state structure of the studied compound.

2.3. Hirshfeld surface analysis

Crystal Explorer 17.5 program employed for the topology analyses [34].

2.4. Computational methods

All software [35-39] utilized in this computational study have been provided in the Supplementary data.

3. Results

3.1. Synthesis of **2**

3-(1*H*-Indol-2-yl)-7*H*-[1,2,4]triazolo[3,4-*b*][1,3,4]thiadiazin-6-ol **2** was obtained in high yield from the reaction of 4-amino-5-(1*H*-indol-2-yl)-1,2,4-triazol-3(2*H*)-thione **1** with ethyl chloroacetate or *tert*-butyl bromoacetate in ethanol and K_2CO_3 as basic condition (Scheme 1). The product was found in the solid state in the enol configuration. The chemical feature of the solid compound elucidated unambiguous by single crystal x-ray diffraction technique combined with a set of spectrophotometric techniques including NMR, Uv-Vis and mass spectra.

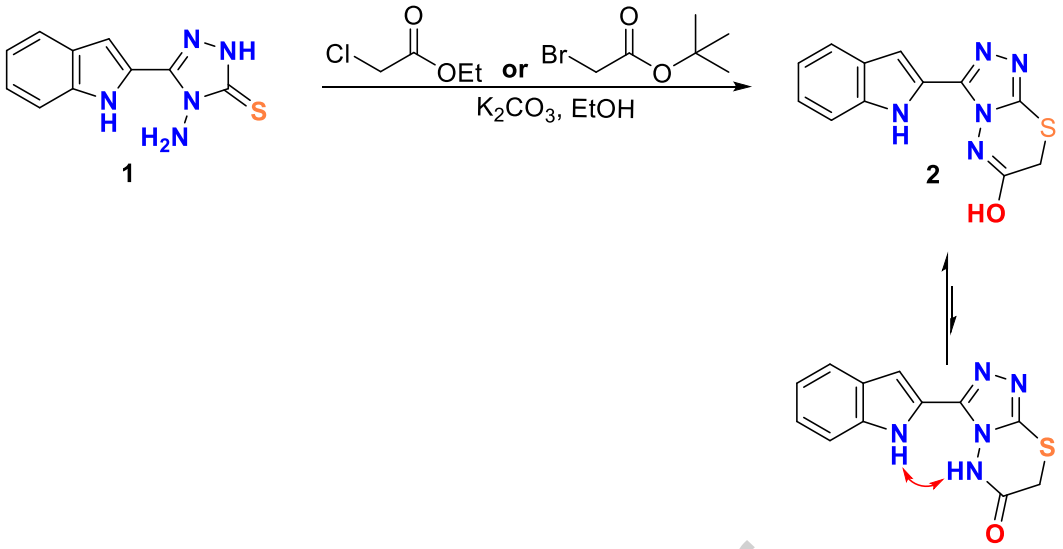

Scheme 1. Synthesis of the

3-(1*H*-indol-2-yl)-7*H*-[1,2,4]triazolo[3,4-*b*][1,3,4]thiadiazin-6-ol **2**

3.2. Structural Characterization

^{1}H NMR spectra shown the two hydrogen adjacent to sulphur atom of the thiadiazine ring at δ 3.92 ppm, the five hydrogen of the indole scaffold shown between 7.02-7.66 ppm, the NH of indole ring appeared at 11.90 ppm and the HO attached to thiadiazine ring was found at 12.68 ppm. ^{13}C NMR spectra showed the methylene carbon at 27.60 ppm, the indole CH carbons appeared at 102.89, 111.88, 119.77, 120.95 and 123.18 ppm. The following signals δ 122.95, 127.47, 136.71, 143.30, 144.61 and 164.23 ppm were assigned for the quaternary carbons. The correlation between vicinal protons or protons and directly attached carbons confirmed by COSY and 2D HMQC respectively (see Supplementary data).

3.3. X-Ray structure descriptions

The solid state X-ray structure of **2** is depicted in Figure 1. It crystallized in the orthorhombic crystal system and Pbca space group with four molecules per unit cell. The unit cell parameters are a = 13.6036(3) Å, b = 7.8245(3) Å, c = 21.3279(8) Å and α= β= γ =90°. The two fused rings of the indole moiety are nearly planar where the angle between the mean planes of the two fused rings is only 2.85°. In addition, the triazole moiety is slightly twisted from the mean plane of the indole moiety by 9.25°. On other hand, the five atoms of the triazole moiety are in the same plane where if we assumed that the S1 and N1 atoms lying above this plane by 0.059 and 0.155 Å, respectively, the C1 atom is located below this plane by 0.649 Å. Further structural details are listed in Tables S1-S6 (Supplementary data).

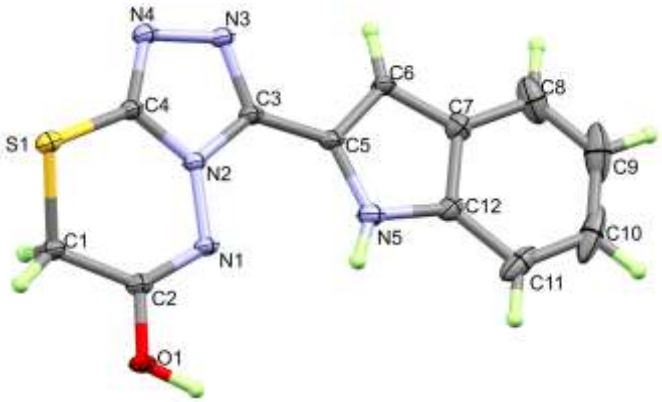

Figure 1. ORTEP for **2**.

The structure of **2** is packed by a number of N...H and O...H hydrogen bonds. The most important hydrogen bond contacts are shown in the left part of Fig. 2 while the hydrogen bond parameters are collected in Table 2. The solid-state structure are packed in the three dimension by O(1)-H(1)...N(4), O(1)-H(1)...N(3), C(6)-H(6)...O(1), and C(1)-H(1B)...N(4) hydrogen bonds with donor-acceptor distances of 3.529(3), 2.518(3), 2.990(3), and 3.303(4)Å, respectively. Packing of the molecular units of **2** is shown in Fig. 2 (right part).

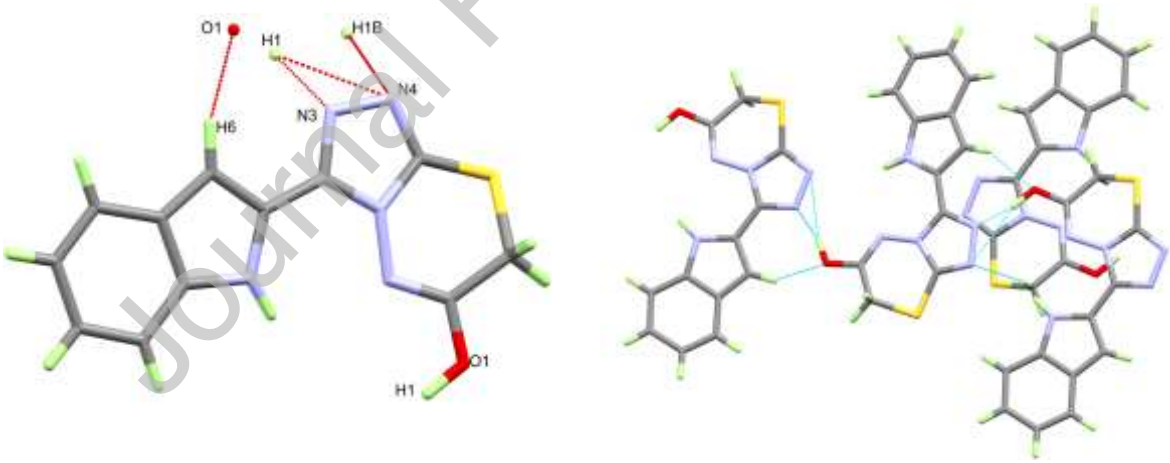

Figure 2. Hydrogen bond contacts (left) and hydrogen bond network (right) in **2**.

Table 1. Crystal Data.

	2
empirical formula	$C_{24}H_{18}N_{10}O_2S_2$
fw	542.60
λ(Å)	1.54184
temp (K)	120(2)
cryst syst	Orthorhombic
space group	Pbca
a (Å)	13.6036(3)
b (Å)	7.8245(3)
c (Å)	21.3279(8)
V (Å^3)	2270.17(13)
Z	4
μ(Mo Kα) (mm^{-1})	2.546
ρ_{calc} (Mg/m^3)	1.588
No. reflns.	9403
GOOF (F^2)	1.117
Unique reflns.	2380
R_{int}	0.0426
R_1[a] ($I \geq 2\sigma$)	0.0613
wR_2[b] ($I \geq 2\sigma$)	0.1622
CCDC	2023823

[a] $R1 = \Sigma||F_o| - |F_c||/\Sigma|F_o|$. [b] $wR2 = [\Sigma[w(F_o^2 - F_c^2)^2]/ \Sigma[w(F_o^2)^2]]^{1/2}$.

Table 2. Hydrogen bonds for **2**[Å and °].

D-H...A	d(D-H)	d(H...A)	d(D...A)	<(DHA)
O(1)-H(1)...N(4)#1	0.96	2.59	3.529(3)	165.6
O(1)-H(1)...N(3)#1	0.96	1.58	2.518(3)	165.6
C(6)-H(6)...O(1)#2	0.95	2.18	2.990(3)	142.6
C(1)-H(1B)...N(4)#3	0.99	2.43	3.303(4)	146.4

Symmetry transformations used to generate equivalent atoms:

#1 x+1/2,-y+1/2,-z+1 #2 x-1/2,-y+1/2,-z+1 #3 -x+1/2,y-1/2,z

3.4. Analysis of molecular packing

The Hirshfeld surfaces of the studied compound are shown in **Fig. 3**. Hirshfeld calculations are important to quantify each intermolecular contact that held the molecular units in the crystal structure. It is clear that the molecular units are held together by many types of intermolecular contacts. The percentage of all representative contacts are drawn in **Fig.4**. The most abundant contacts are the H…H, N…H, H…C(π) and S…H interactions. On other hand, the most significant contacts are those presented in **Figs. 5** and **6** which comprised the decomposed fingerprint plots and d_{norm} maps of these interactions. All the N…H, H…C(π), O…H, and C…C contacts appeared as red areas in the corresponding d_{norm} maps which confirm that these interactions have shorter distances than the vdW radii sum of the interacting atoms. Summary of the short intermolecular contacts as well as the corresponding interaction distances as acquired from the Hirshfeld calculations are summarized in **Table 3**. Small amount of C…C contacts (1.9%) was detected with shortest C…C distance of 3.162 Å for the C2…C11 contact leave no doubt on the presence of some π-π interactions. In addition, Hirshfeld calculations revealed the presence of some S…H contacts slightly shorter (3.476 Å) than the vdW radii sum of the S and H atoms.

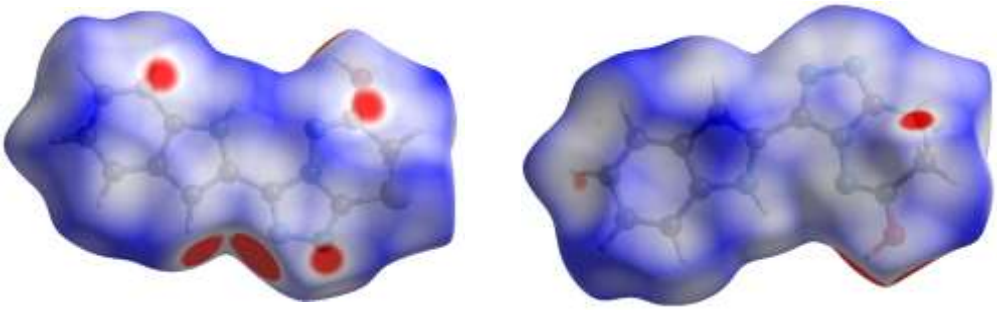

d_{norm}

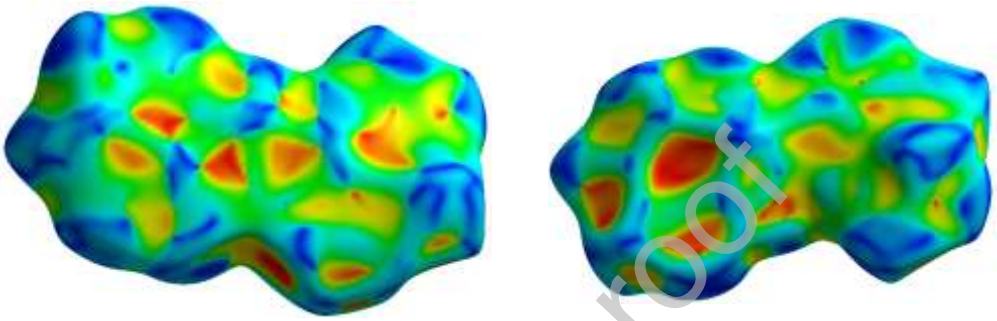

Shape index

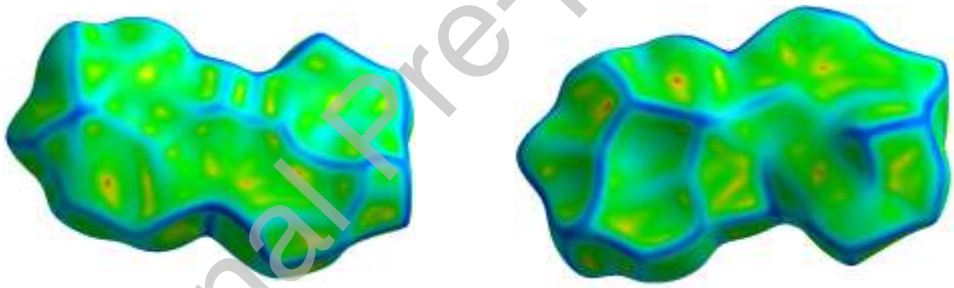

Curvedness

Figure 3. Hirshfeld surfaces of **2**.

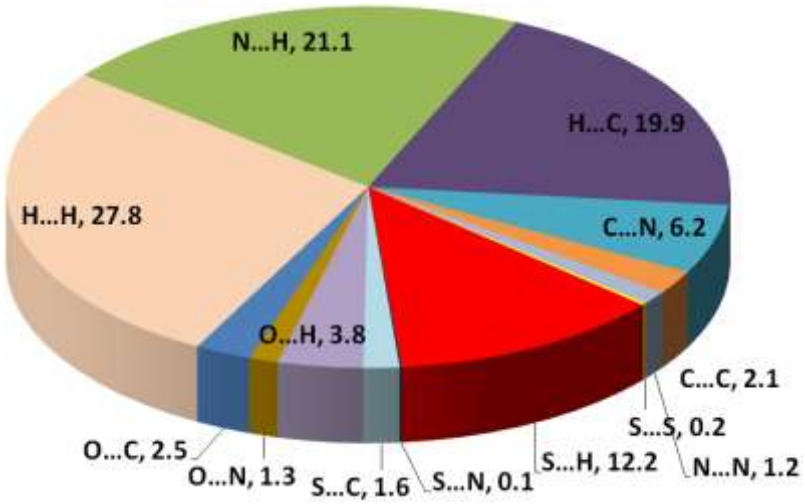

Figure 4. All intermolecular interactions summary of the studied compound **2**.

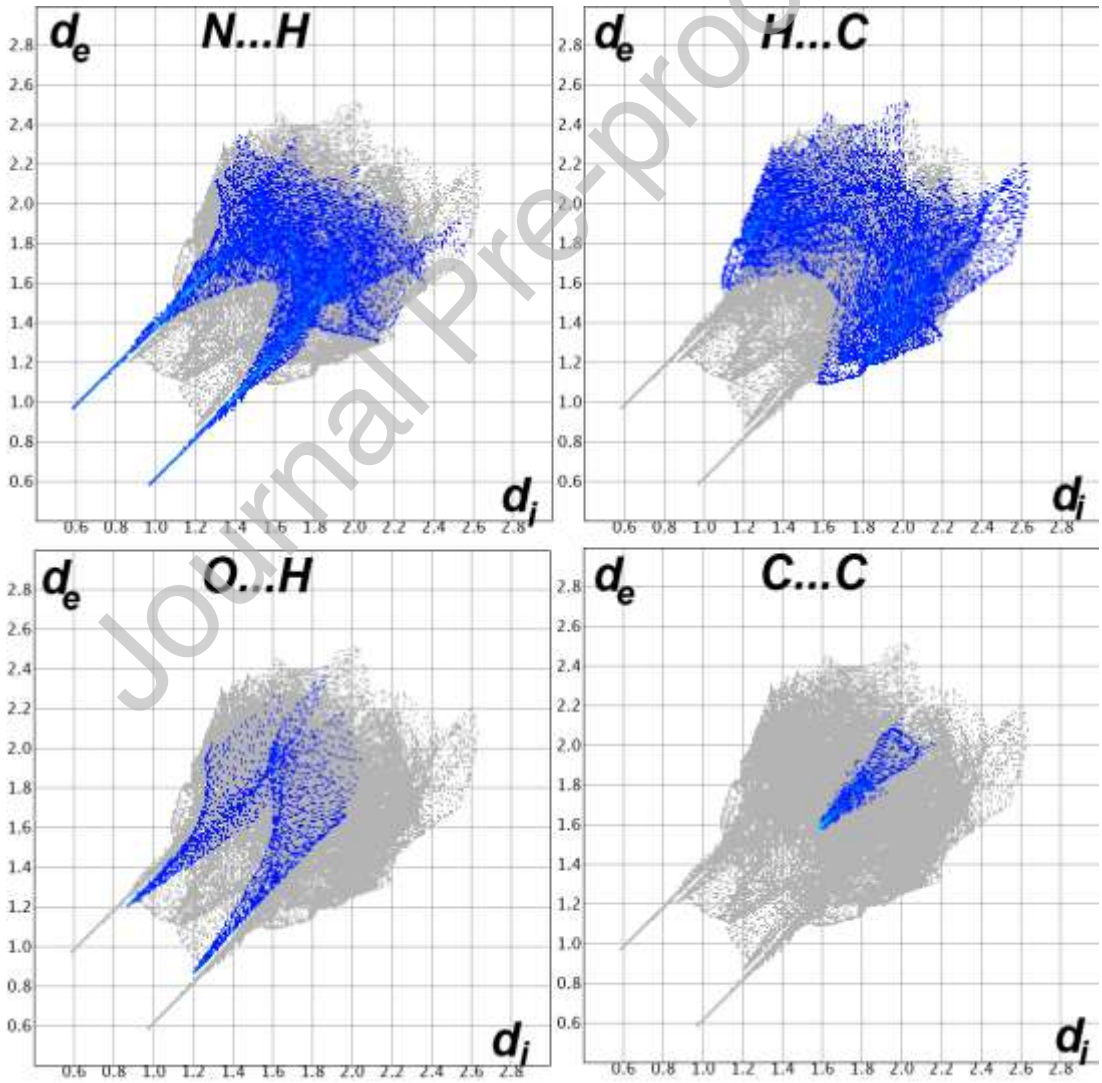

Figure 5. Fingerprint plots of the most important intermolecular interactions in **2**.

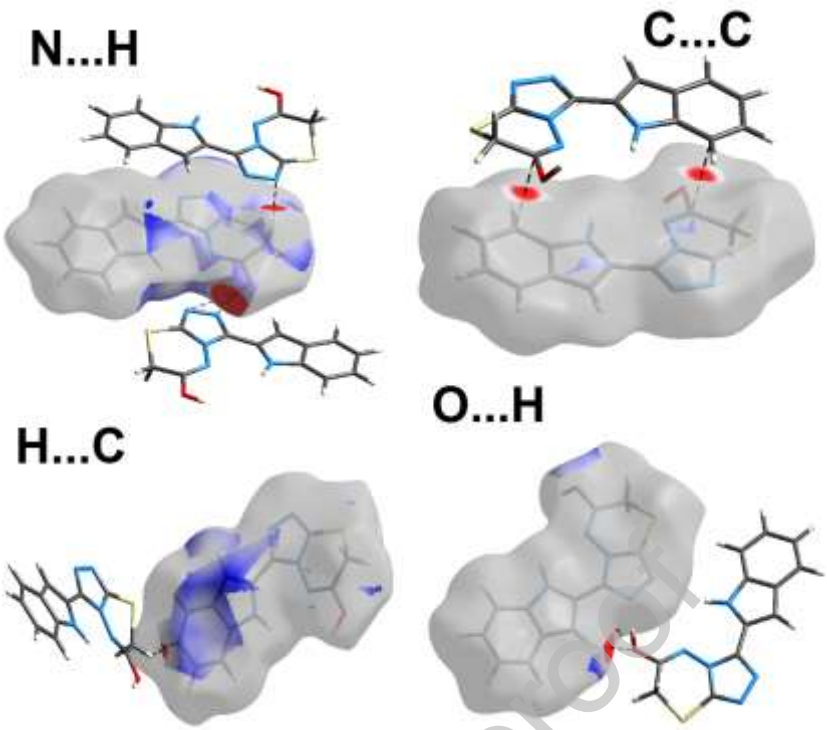

Figure 6. The d_{norm} maps of the most important intermolecular interactions in **2**.

Table 3. Summary of all short contacts and the interaction distances.

Contact	Distance	Contact	Distance
O1…H6	2.075	N4…H1B	2.356
N3…H1	1.555	C9…H1A	2.684
N4…H1	2.569	C2…C11	3.164
S1...C8	3.476		

3.5. DFT studies

The calculated molecular structure of **2** as well as the structure match between the experimental and calculated are depicted in **Fig. 7**. It was observed that both structures are very close to each other. There are also good squarely interrelationship among the bond angles and bond distances of the experimental and computed study of the compound **2** (**Fig. 8**). The Cartesian coordinates of the optimized structure as well as the bond angles and distances compared to the acquired results experimentally are given in **Table S7** (Supplementary data).

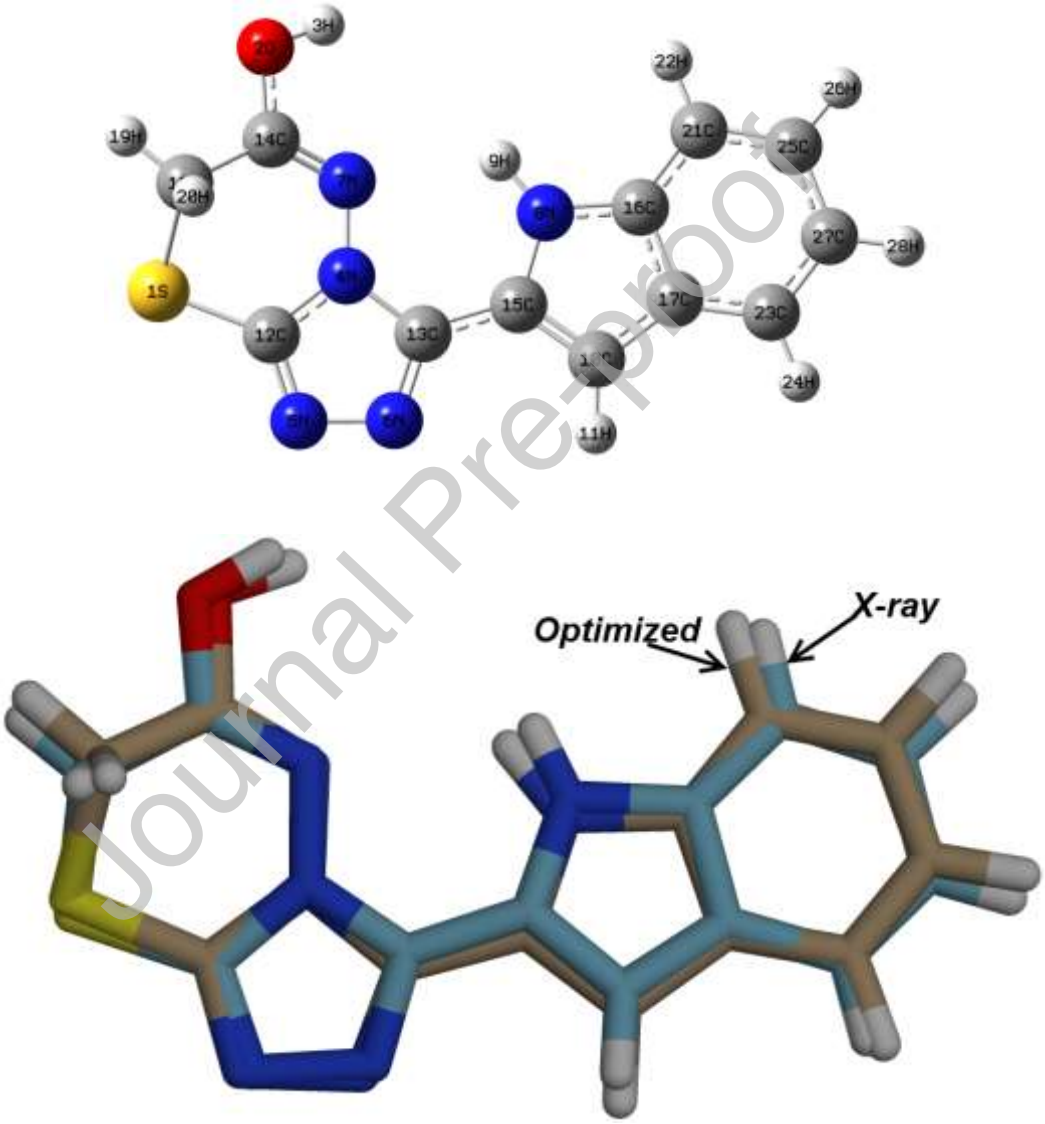

Figure 7. The geometry optimized (upper) and overlay of the solid-state x-ray structure with the optimized geometry (lower) for **2**.

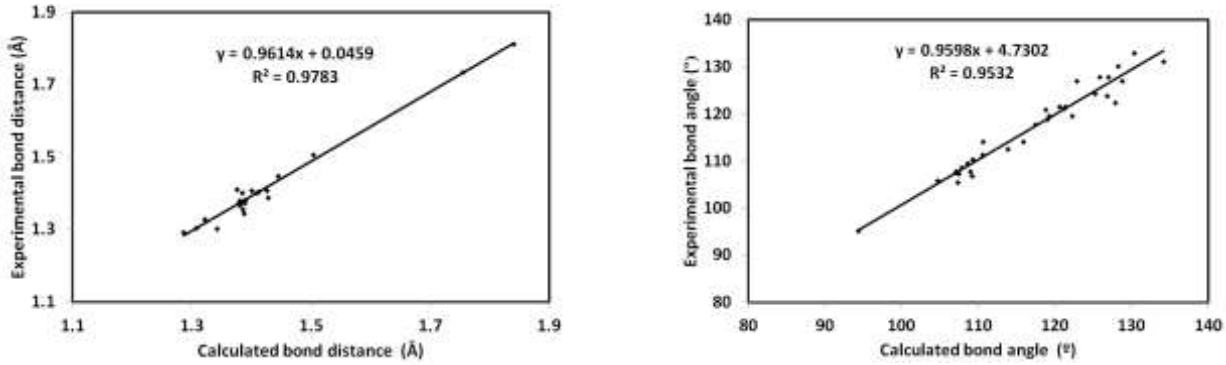

Figure 8. The straight line correlations between the calculated and experimental geometric parameters.

Table 4 are summarized the natural charges acquired by NBO calculation. It is clear that the most electropositive sites are the O-H (0.5109) and N-H (0.4472) protons as well as the carbon atoms (0.6018) located between N and O as strong electronegative atoms and sulphur atom as well (0.3483). On other hand, all N (-0.2472 to -0.5555) and O (-0.6733) atomic sites have the highest negative natural charge. Presentation of the molecular electrostatic potential (MEP) mapped over electron density showing the dipole moment vector is presented in **Fig. 9**. There are red and blue areas representing the most electron rich and electron poor sites in **2,** respectively. These atomic sites are most reactive site to be attacked by an electrophile and nuclceophile, respectively.

Table 4. Natural atomic charges of **2**[a].

Atom	Charge	Atom	Charge	Atom	Charge
S1	0.3483	C10	-0.2490	H19	0.2955
O2	-0.6733	H11	0.2636	H20	0.2821
H3	0.5109	C12	0.1410	C21	-0.2728
N4	-0.2472	C13	0.3426	H22	0.2357
N5	-0.2883	C14	0.6018	C23	-0.2127
N6	-0.2817	C15	0.0997	H24	0.2414
N7	-0.3873	C16	0.1666	C25	-0.2373
N8	-0.5555	C17	-0.1004	H26	0.2389
H9	0.4472	C18	-0.6884	C27	-0.2608

[a]Atom numbering refer to **Fig. 7**

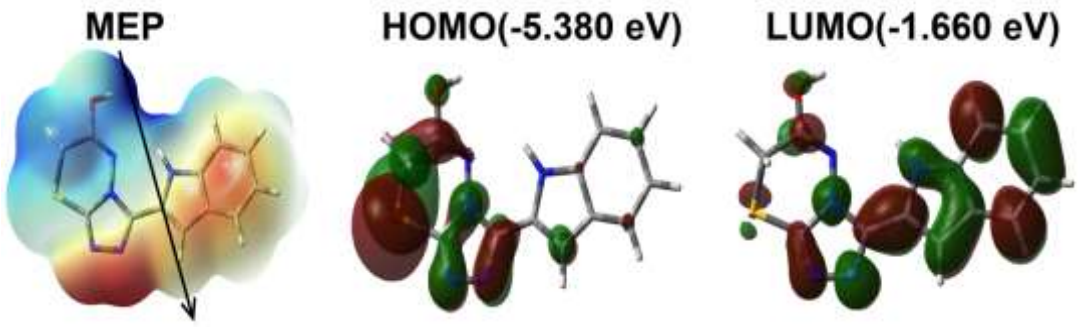

Figure 9. The MEP, HOMO and LUMO of **2**.

To study the reactivity of the molecule, the frontier molecular orbitals (HOMO, and LUMO) were computed [41-47]. Their energies were computed and acquired to be -5.380 and -1.660 eV, respectively. Hence, the computed electron affinity (A), and ionization potential (I) are 1.6605, and 5.380 eV, respectively. Also, the electrophilicity index, and hardness are -3.262 and 3.720, 3.520 eV, respectively. The HOMO level is located over the fused triazole ring system and it represents the most favored area from which the electronic transition could occur. On other hand, the LUMO is distributed over most of the π-system. Hence, the HOMO to LUMO excitation represent mixed n-π* and π-π* transitions. The energy needed for this intermolecular charge transfer is 3.720 eV.

3.6. NBO analysis

The conjugation system play a crucial role in the electron delocalization processes from occupied orbitals to antibonding empty orbitals [48, 49]. These electron delocalization processes and the corresponding stabilization energies ($E^{(2)}$) are summarized in **Table 5**. The compound is settled by a number of σ-σ*, n→σ*, n→π*, and π→π* intramolecular charge transfer (IMCT) processes. These IMCT processes stabilized the system up to 7.73, 32.13, 12.15 and 43.34 kcal/mol, respectively.

Table 5: The $E^{(2)}$ (kcal/mol) values for the charge transfer interactions in **2**[a].

Donor NBO	**Acceptor NBO**	**$E^{(2)}$**	**Donor NBO**	**Acceptor NBO**	**$E^{(2)}$**
σ→σ*			**π→π***		
σ(O2-H3)	σ*(C14 -C18)	5.46	π(N5-C12)	π*(N6-C13)	11.90
σ(N4-N7)	σ*(O2 -C14)	4.67	π(N6-C13)	π*(N5-C12)	15.27
σ(N4-C13)	σ*(S1 -C12)	4.66	π(N6-C13)	π*(C10-C15)	9.45
σ(N5-N6)	σ*(S1 -C12)	7.73	π(N8-C16)	π*(C10-C15)	20.48
σ(N5-N6)	σ*(C13 -C15)	5.55	π(N8-C16)	π*(C21-C25)	5.39
σ(N8-C15)	σ*(C16 -C21)	4.51	π(C10-C15)	π*(N6-C13)	19.41
σ(C10-C15)	σ*(C17-C23)	5.37	π(C10-C15)	π*(N8-C16)	7.35
σ(C10-C17)	σ*(C13-C15)	6.24	π(C21-C25)	π*(N8-C16)	32.13
σ(C21-C25)	σ*(N8-C16)	6.17	π(C21-C25)	π*(C23-C27)	16.63
σ(C23-C27)	σ*(C10-C17)	4.56	π(C23-C27)	π*(C21-C25)	19.61
n→σ*			**n→π***		
n(O2)	σ*(N7-C14)	6.50	n(S1)	π*(N5-C12)	17.53
n(N5)	σ*(N4-C12)	9.14	n(O2)	π*(N7-C14)	43.34
n(N5)	σ*(N6-C13)	5.60	n(N4)	π*(N5-C12)	41.86
n(N5)	σ*(N4-C12)	9.14	n(N4)	π*(N6-C13)	40.66
n(N5)	σ*(N6-C13)	5.60	n(N4)	π*(N7-C14)	22.07
n(N6)	σ*(N4-C13)	8.67			
n(N6)	σ*(N5-C12)	5.58			
n(N7)	σ*(O2-C14)	4.87			
n(N7)	σ*(N4-C12)	8.78			
n(N7)	σ*(N8-H 9)	4.47			
n(N7)	σ*(C14-C18)	12.15			

[a]Atom numbering refer to **Fig. 7**

3.7. UV-Vis and NMR spectra

The results acquired for the UV-Vis electronic spectra of **2** experimentally in EtOH exhibited a broad absorption band at 313 nm and two shoulders at 333 and 309 nm (**Fig. 10**). Their assignments showing the molecular orbitals included in these electronic transitions are listed in **Table 6** and shown in **Fig. 11**. The TD calculations predicted these transitions at 310.6 nm (f=0.071), 347.5 nm (f=0.420) and 285.4 nm (f=0.311), respectively which corresponding to H-1→LUMO, HOMO→LUMO (96%) and HOMO→L+1 (89%), respectively.

Table 6. The electronic spectra assignment of **2**.

No.	$(\lambda_{max})_{calc}$	f_{osc} [a]	Assignment	$(\lambda_{max})_{observ}$
I	347.5	0.420	HOMO→LUMO (96%)	333
II	310.6	0.071	H-1→LUMO (96%)	313
III	285.4	0.311	HOMO→L+1 (89%)	309

[a] oscillator strength

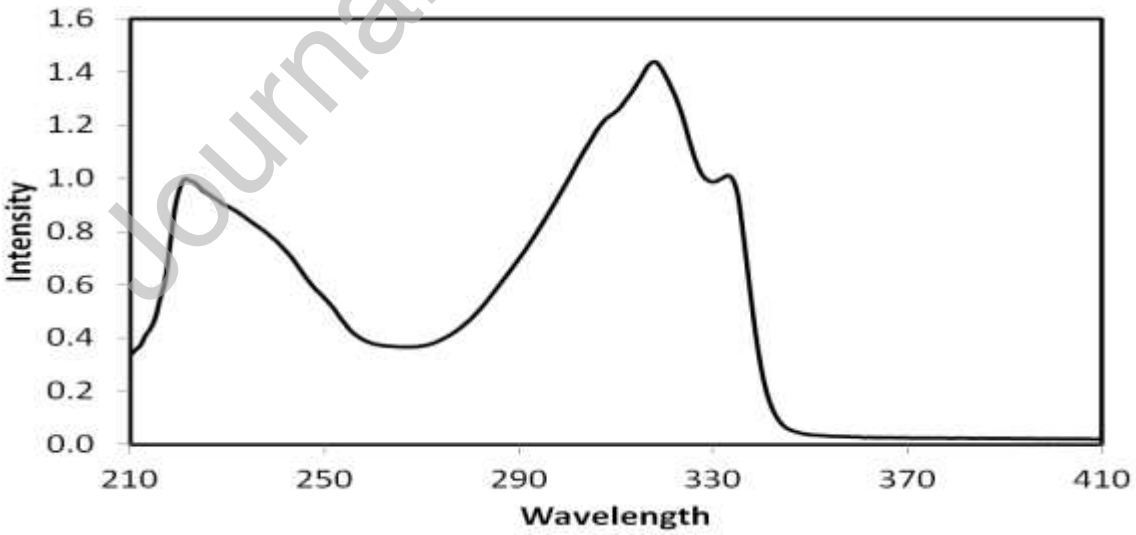

Figure 10. The UV-Vis spectra of **2** in ethanol.

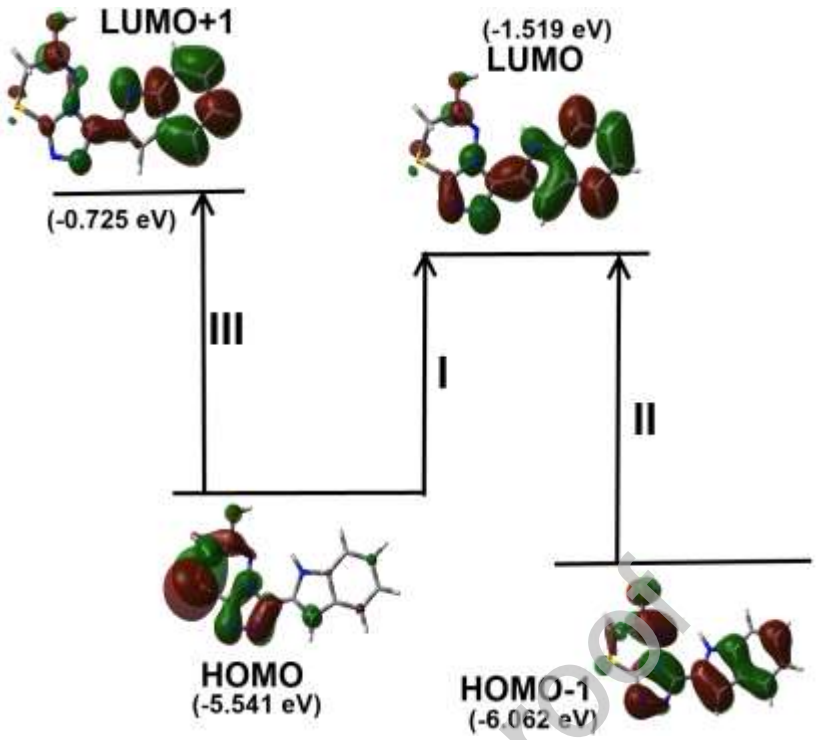

Figure 11. Origin of the UV-Vis spectral bands of **2** in ethanol as solvent. The definition of **I**, **II** and **III** refer to **Table 6**.

Table S8 provided in the Supplementary data summarized the computed of the ^{1}H and ^{13}C chemical shifts (C.S) and the results acquired experimentally. It is clear from **Fig. 12** that there are also good squarely interrelationship among the computed C.s and the results acquired experimentally. The correlation coefficients are 0.9455, and 0.9969 for ^{1}H-NMR, and ^{13}C-NMR respectively.

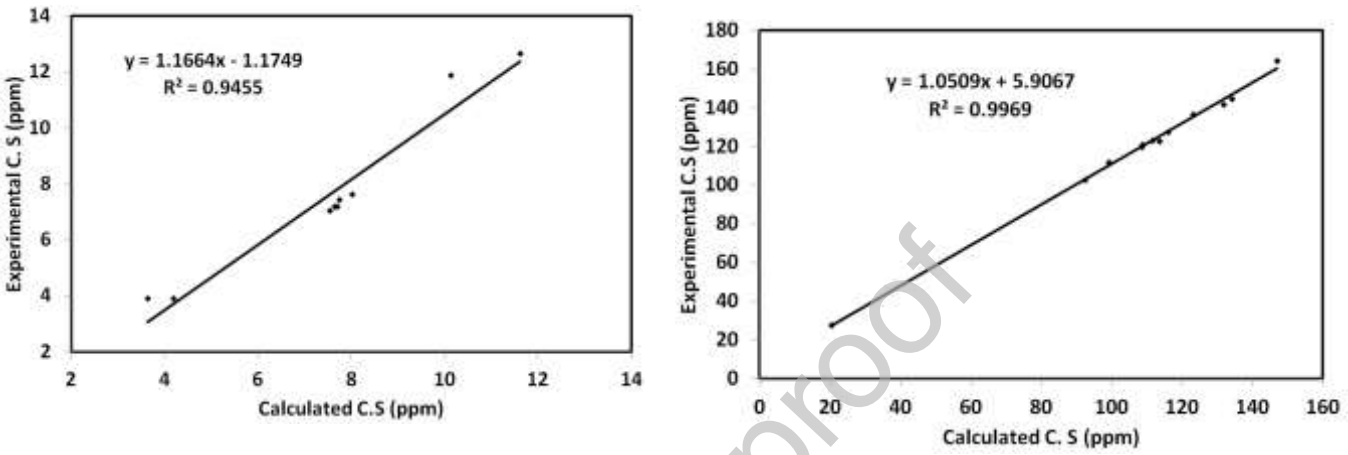

Figure 12. Correlation graphs of the ^{1}H and ^{13}C NMR chemical shifts between the computed and results acquired experimentally

3.8. Tautomerism in 2

The studied molecule could exist in the two possible tautomeric structures shown in **Fig. 13**. The geometry optimizations and frequency calculations for both tautomers allowed us to compute their energies and thermodynamic parameters. Energetically both tautomers have very close energies and thermodynamic parameters (**Table 7**). The keto form is energetically higher than the enol form by only 2 kcal/mol either in the gas phase or in solution of the compound in DMSO as solvent using B3LYP/6-31G(d,p) method. The thermodynamic parameters listed in **Table 7** confirmed that the enol form is the thermodynamically most stable for the studied compound. The higher energies of the keto form may be attributed to the presence of some steric between the two N-H protons. Although, the results are in good agreement with the experimentally observed X-ray structure but still there is a possibility for the existence of equilibrium among the two tautomers in solution.

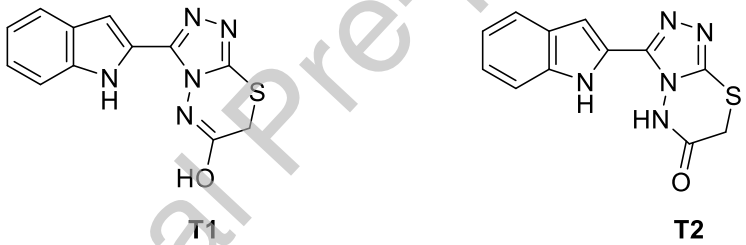

Figure 13. Structure of the two suggested tautomers of the studied molecule.

Table 7. Energetic of both tautomers in gas phase and in solution of the compound in DMSO as solvent.

Parameter	**T1**	**T2**	**T1**	**T2**
	Gas		**DMSO**	
E	-1209.8334	-1209.8304	-1209.8542	-1209.8511
ZPVE	0.2044	0.2039	0.2045	0.2041
E_{corr}[a]	-1209.6291	-1209.6265	-1209.6497	-1209.6471
ΔE		1.6146		1.6146
H	-1209.6137	-1209.6109	-1209.6344	-1209.6313
S	121.6520	123.4450	121.3320	124.4010
G	-1209.6715	-1209.6695	-1209.6920	-1209.6904

4. Conclusions

The target compound 3-(1*H*-indol-2-yl)-7*H*-[1,2,4]triazolo[3,4-*b*][1,3,4]thiadiazin-6-ol **2** was synthesized in excellent yield from coupling of triazolyl-indole derivative **1** and alkyl halo-ester using K_2CO_3 as a base. DFT calculations were used to analyze the ket-enol tautomerism in the studied system. It is found that the enol form which is observed experimentally is more stable than the keto form. Its supramolecular structure is quantitatively analyzed using Hirshfeld calculations. Also, calculated NMR and Uv-Vis spectra are in good agreement with the experimental data.

Author Contributions: Conceptualization, A.T.A.B., and A.B.; Methodology, and Investigation, A.T.A.B.; Formal analysis, and Data curation, A.T.A.B., M.H., and S.M.S.; Software, M.H.; Visualization, and funding acquisition: A.B.; A.B. Writing – original draft, A.T.A.B., M.H., S.M.S. and A.B. All authors approved the final version.

Funding: The authors would like to extend their sincere appreciation to the Researchers Supporting project number (RSP-2020/64), King Saud University, Riyadh, Saudi Arabia.

Acknowledgments: The authors would like to extend their sincere appreciation to the Researchers Supporting project number (RSP-2020/64), King Saud University, Riyadh, Saudi Arabia.

Conflicts of Interest: The authors declare no conflict of interest.

References

1. Shiradkar, M.; Kumar, G.V.S.; Dasari, V.; Tatikonda, S.; Akula, K.C.; Shah, R., Clubbed triazoles: a novel approach to antitubercular drugs. *Eur. J. Med. Chem.* **2007**, *42*(6), 807-816.
2. Almasirad, A.; Tabatabai, S.A.; Faizi, M.; Kebriaeezadeh, A.; Mehrabi, N.; Dalvandi, A.; Shafiee, A., Synthesis and anticonvulsant activity of new 2-substituted-5-[2-(2-fluorophenoxy) phenyl]-1, 3, 4-oxadiazoles and 1, 2, 4-triazoles. *Bioorg. Med. Chem. Lett.***2004**. *14*(24), 6057-6059.
3. Patil, S.A.; Manjunatha, M.; Kulkarni, A.D.; Badami, P.S., Synthesis, characterization, fluorescence and biological studies of Mn (II), Fe (III) and Zn (II) complexes of Schiff bases derived from isatin and 3-substituted-4-amino-5-mercapto-1, 2, 4-triazoles. *Complex Met.***2014**. *1*(1), 128-137.
4. El Sayed, H.; Awad, L.F.; Soliman, S.M.; Abd Al Moaty, M.N.; Ghabbour, H.A.; Barakat, A., Tautomerism aspect of thione-thiol combined with spectral investigation of some 4-amino-5-methyl-1, 2, 4-triazole-3-thione Schiff's bases. *Journal of Molecular Structure*, **2017**, *1146*, 432-440.
5. Bai, Y.; Zhao, G.; Li, C.; Zhao, S.; Shi, Z., Microwave-enhanced reactions of 4-amino-5-merecapto-1, 2, 4-triazoles with benzoyl chloride and aromatic aldehydes. *Synth. Commun.* **2008**, *38*(19), 3311-3319.
6. Riyadh, S.M.; Gomha, S.M., Two decades of the synthesis of mono-and bis-aminomercapto [1, 2, 4] triazoles. *RSC Advances*, **2020**, *10*(42), 24994-25012.
7. Gomha, S.M.; Abdel-aziz, H.M.; Abolibda, T.Z.; Hassan, S.A.; Abdalla, M.M., Green synthesis, molecular docking and pharmacological evaluation of new triazolo-thiadiazepinylcoumarine derivatives as sedative hypnotic scaffold. *J. Heterocycl. Chem.,* **2020,** *57*(3), 1034-1043.
8. Abdallah, M.A.; Riyadh, S.M.; Abbas, I.M.; Gomha, S.M., Synthesis and Biological Activities of 7-Arylazo-7H-pyrazolo [5, 1-c][1, 2, 4] Triazol-6 (5H)-Ones and

7-Arylhydrazono-7H-[1, 2, 4] triazolo [3, 4-b][1, 3, 4] thiadiazines. *J. Chin. Chem. Soc.*, **2005**, *52*, 987-994.

9. Jiang, B.; Huang, X.; Yao, H.; Jiang, J.; Wu, X.; Jiang, S.; Wang, Q.; Lu, T.; Xu, J., Discovery of potential anti-inflammatory drugs: diaryl-1, 2, 4-triazoles bearing N-hydroxyurea moiety as dual inhibitors of cyclooxygenase-2 and 5-lipoxygenase. *Organic & biomolecular chemistry*, **2014,** *12*(13), 2114-2127.
10. Boraei, A.T.A.; Gomaa, M.S.; El Sayed, E.S.H.; Duerkop, A. Design, selective alkylation and X-ray crystal structure determination of dihydro-indolyl-1,2,4-triazole-3-thione and its 3-benzylsulfanyl analogue as potent anticancer agents. *Eur. J. Med. Chem.* **2017**, *125*, 360–371.
11. Boraei, A.T.A.; Singh, P.K.; Sechi, M.; Satta, S. Discovery of novel functionalized 1, 2, 4-triazoles as PARP-1 inhibitors in breast cancer: Design, synthesis and antitumor activity evaluation. *Eur. J. Med. Chem.* **2019**, *182*, 111621.
12. Chu, Q.-Z.; Zhou, H.-R.; Zhang, X.-R. 3-benzyl-sulfanyl-5-(4-phenyl-1H-1,2,3-triazol-1-ylmeth-yl)-4H-1,2,4-triazol-4-amine. *Acta Cryst.* **2008**, *E64*, o1611.
13. Boraei, A.T.A.; Sarhan, A.A.M.; Yousuf, S.; Barakat, A. Synthesis of a New Series of Nitrogen/Sulfur Heterocycles by Linking Four Rings: Indole; 1,2,4-Triazole; Pyridazine; and Quinoxaline. *Molecules* **2020**, *25*, 450.
14. Sarhan, A.A.; Boraei, A.T.A.; Barakat, A.; Nafie, M.S. Discovery of hydrazide-based pyridazino [4–b] indole scaffold as a new phosphoinositide 3-kinase (PI3K) inhibitor for breast cancer therapy. *RSC Advances* **2020**, *10*, 19534–19541.
15. Boraei, A.T.A.; Ghabbour, H.A.; Gomaa, M.S.; El Ashry, E.S.H.; Barakat, A. Synthesis and anti-proliferative assessment of triazolo-thiadiazepine and triazolo-thiadiazine scaffolds. *Molecules* **2019**, *24*, 4471.
16. Badria, F.A.; Soliman, S.M.; Atef, S.; Islam, M.S.; Al-Majid, A.M.; Dege, N.; Ghabbour, H.A.; Ali, M.; El-Senduny, F.F.; Barakat, A. Anticancer Indole-Based Chalcones: A Structural and Theoretical Analysis. *Molecules* **2019**, *24*, 3728.
17. Boraei, A.T.; El Ashry, E.S.H.; Barakat, A.; Ghabbour, H.A. Synthesis of new functionalized indoles based on ethyl indol-2-carboxylate. *Molecules* **2016**, *21*, 333.
18. Boraei, A.T. A new direct synthetic access to 4-Amino-2-N-(glycosyl/propyl)-1,2,4-triazole-3-thiones via hydrazinolysis of

3-N-((Acylated gylcosyl)/allyl)-1,3,4-oxadiazole-2-thiones. *Arkivoc* **2016**, *iii*, 71–81.

19. Abdelhameed, R.M.; El-Sayed, H.A.; El-Shahat, M.; El-Sayed, A.A.; M.; Darwesh, O. Novel triazolothiadiazole and triazolothiadiazine derivatives containing pyridine moiety: Design, synthesis, bactericidal and fungicidal activities. *Curr. Bioact. Compd.* **2018**, *14*, 169–179.
20. Kaur, R.; Dwivedi, A.R.; Kumar, B.; Kumar, V. Recent developments on 1, 2, 4-triazole nucleus in anticancer compounds: A review. *Anti-Cancer Agent. Med. Chem.* **2016**, *16*, 465–489.
21. Ayati, A.; Emami, S.; Foroumadi, A. The importance of triazole scaffold in the development of anticonvulsant agents. *Eur. J. Med. Chem.* **2016**, *109*, 380–392.
22. Amer, A.; Ayoup, M.S.; Khattab, S.N.; Hassan, S.Y.; Langer, V.; Senior, S.; El Massry, A.M. A regio-and stereo-controlled approach to triazoloquinoxalinyl C-nucleosides. *Carbohydr. Res.* **2010**, *345*, 2474–2484.
23. Keri, R.S.; Patil, S.A.; Budagumpi, S.; Nagaraja, B.M. Triazole: A Promising Antitubercular Agent. *Chem. Biol. Drug Des.* **2015**, *86*, 410–423.
24. Ayoup, M.S.; Ahmed, H.E.A.; El Massry, A.M.; Senior, S.; Khattab, S.N.; Hassan, S.Y.; Amer, A. Synthesis, Docking, and Evaluation of Antimicrob. Activity of a New Series of Acyclo C-Nucleosides of 1,2,4-Triazolo [4, 3-a] quinoxaline Derivatives. *J. Heterocycl. Chem.* **2016**, *53*, 153–163.
25. Boraei, A.T.; Soliman, S.M.; Yousuf, S.; Barakat, A., Synthesis Single Crystal X-ray Structure DFT Studies and Hirshfeld Analysis of New Benzylsulfanyl-Triazolyl-Indole Scaffold. *Crystals*, **2020,** *10*(8), p.685.
26. Wang, W.; Hellinga, H. W.; Beese, L. S. Structural Evidence for the Rare Tautomer Hypothesis of Spontaneous Mutagenesis. Proc. Natl. Acad. Sci. U. S. A. 2011, 108, 17644.
27. Harisha, R.S.; Hosamani, K.M.; Keri, R.S., Synthesis, in-vitro Microbial and Cytotoxic Studies of New Benzimidazole Derivatives. *Archiv der Pharmazie: An International Journal Pharmaceutical and Medicinal Chemistry*, **2009,** *342*(7), 412-419.

28. Kidwai, M.; Mothsra, P., Microwave-assisted neat reaction technology for the synthesis of s-triazolo [3, 4-b]-1, 3, 4-thiadiazines. *Journal of Sulfur Chemistry*, **2007,** *28*(2), 149-153.
29. Moustafa, O.S., 2000. Bridgehead Nitrogen Heterocycles: Synthesis and Reactions of S-Triazolothiadiazinyl and S-Triazolothiadiazo-Lylquinoxalines. *Phosphorus, Sulfur, and Silicon and the Related Elements*, *167*(1), pp.101-110.
30. El Ashry, E. S. H.; Kassem, A. A.; Abdel-Hamid, H.; Louis, F. F.; Khattab, Sh. A. N.; Aouad, M. R. Synthesis of 4-amino-5-(3-chlorobenzo[b]thien-2-yl)-3-mercapto1,2,4-triazolo[3,4-b][1,3,4]thiadiazoles and triazolo[3,4,b][1,3,4]thiadiazines under classical and microwave conditions. ARKIVOC 2006 (xiv) 119-132.
31. Rikagu Oxford Diffraction. *CrysAlisPro*; Agilent Technologies inc.: Yarnton, Oxfordshire, UK, 2018.
32. Sheldrick, G.M. SHELXT–Integrated space-group and crystal-structure determination. *Acta Cryst.* **2015**, *C71*, 3–8.
33. Hübschle, C.B.; Sheldrick, G.M.; Dittrich, B. ShelXle: A Qt graphical user interface for SHELXL. *J. Appl. Cryst.* **2011**, *44*, 1281–1284.
34. Turner, M.J.; McKinnon, J.J.; Wolff, S.K.; Grimwood, D.J.; Spackman, P.R.; Jayatilaka, D.; Spackman, M.A. Crystal Explorer17 (2017) University of Western Australia. Available online: http://hirshfeldsurface.net. (Accessed on 12 June 2017).
35. Frisch, M.J.; Trucks, G.W.; Schlegel, H.B.; Scuseria, G.E.; Robb, M.A.; Cheeseman, J.R.; Scalmani, G.; Barone, V.; Mennucci, B.; Petersson, G.A.; *et al*. *GAUSSIAN 09*; Revision A02; Gaussian Inc.: Wallingford, CT, USA, 2009
36. *GaussView*; Version 4.1; Dennington II, R., Keith, T., Millam, J., Eds.; Semichem Inc.: Shawnee Mission, KS, USA, 2007.
37. Reed, A.E.; Curtiss, L.A.; Weinhold, F. Intermolecular interactions from a natural bond orbital, donor-acceptor viewpoint. *Chem. Rev.* **1988**, *88*, 899–926.
38. Marten, B.; Kim K.; Cortis, C.; Friesner, R. A.; Murphy, R. B.; Ringnalda, M. N.; Sitkoff, D.; Honig, B. New Model for Calculation of Solvation Free Energies: Correction of Self-Consistent Reaction Field Continuum Dielectric Theory for Short-Range Hydrogen-Bonding Effects, *J. Phys. Chem.* **1996** *100* 11775-11765.

39. Tannor, D.J.; Marten, B.; Murphy, R.; Friesner, R.A.; Sitkoff, D.; Nicholls, A.; Ringnalda, M.; Goddard, W.A.; Honig, B. Accurate first principles calculation of molecular charge distributions and solvation energies from ab initio quantum mechanics and continuum dielectric theory. *J. Am. Chem. Soc.* **1994**, *116*, 11875–11882.
40. Cheeseman, J.R.; Trucks, G.W.; Keith, T.A.; Frisch, M.J. A Comparison of Models for Calculating Nuclear Magnetic Resonance Shielding Tensors. *J. Chem. Phys.* **1996**, *104*, 5497–5509.
41. Foresman, J.B.; Frisch, *Æ*. *Exploring Chemistry with Electronic Structure Methods*; 2nd ed.; Gaussian: Pittsburgh, PA, USA, 1996.
42. Chang, R. *Chemistry*; 7th ed.; McGraw-Hill: New York, NY, USA, 2001.
43. Kosar, B.; Albayrak, C. Spectroscopic investigations and quantum chemical computational study of (E)-4-methoxy-2-[(p-tolylimino) methyl] phenol. *Spectrochim. Acta* **2011**, *78*, 160–167.
44. Koopmans, T.A. Ordering of wave functions and eigenenergies to the individual electrons of an atom. *Physica* **1933**, *1*, 104–113.
45. Parr, R.G.; Yang, W. *Density-Functional Theory of Atoms and Molecules*; Oxford University Press: New York, NY, USA, 1989.
46. Parr, R.G.; Szentpaly, L.V.; Liu, S. Electrophilicity index. *J. Am. Chem. Soc.* **1999**, *121*, 1922–1924.
47. Singh, R.N.; Kumar, A.; Tiwari, R.K.; Rawat, P.; Gupta, V.P. A combined experimental and quantum chemical (DFT and AIM) study on molecular structure, spectroscopic properties, NBO and multiple interaction analysis in a novel ethyl 4-[2-(carbamoyl) hydrazinylidene]-3, 5-dimethyl-1H-pyrrole-2-carboxylate and its dimer. *J. Mol. Strut.* **2013**, *1035*, 427–440.
48. Hubert Joe, I.; Kostova, I.; Ravikumar, C.; Amalanathan, M.; Pinzaru, S.C. Theoretical and vibrational spectral investigation of sodium salt of acenocoumarol." *J. Raman Spectrosc.* **2009**, *40*, 1033–1038.
49. Sebastian, S.; Sundaraganesan, N. The spectroscopic (FT-IR, FT-IR gas phase, FT-Raman and UV) and NBO analysis of 4-Hydroxypiperidine by density functional method. *Spectrochim. Acta Part A Mol. Biomol. Spectrosc*. **2010**, *75*, 941–952.

Graphical abstract